Members of the KCTD family are major regulators of cAMP signaling

Brian S. Muntean[a,b,1], Subhi Marwari[a], Xiaona Li[a], Douglas C. Sloan[b], Brian D. Young[c], James A. Wohlschlegel[c], and Kirill A. Martemyanov[a,1]

[a]Department of Neuroscience, The Scripps Research Institute, Jupiter, FL 33458; [b]Department of Pharmacology and Toxicology, Medical College of Georgia, Augusta University, Augusta, GA 30912; and [c]Department of Biological Chemistry, David Geffen School of Medicine at UCLA, Los Angeles, CA 90095

Edited by David Clapham, HHMI, Janelia Research Campus, Ashburn, VA; received October 26, 2021; accepted November 11, 2021

Cyclic adenosine monophosphate (cAMP) is a pivotal second messenger with an essential role in neuronal function. cAMP synthesis by adenylyl cyclases (AC) is controlled by G protein–coupled receptor (GPCR) signaling systems. However, the network of molecular players involved in the process is incompletely defined. Here, we used CRISPR/Cas9–based screening to identify that members of the potassium channel tetradimerization domain (KCTD) family are major regulators of cAMP signaling. Focusing on striatal neurons, we show that the dominant isoform KCTD5 exerts its effects through an unusual mechanism that modulates the influx of Zn^{2+} via the Zip14 transporter to exert unique allosteric effects on AC. We further show that KCTD5 controls the amplitude and sensitivity of stimulatory GPCR inputs to cAMP production by Gβγ-mediated AC regulation. Finally, we report that KCTD5 haploinsufficiency in mice leads to motor deficits that can be reversed by chelating Zn^{2+}. Together, our findings uncover KCTD proteins as major regulators of neuronal cAMP signaling via diverse mechanisms.

cAMP | GPCR | neuron | striatum | zinc

Cyclic adenosine monophosphate (cAMP) is the key second messenger that mediates a vast number of cellular reactions to oncoming stimuli (1). Accordingly, it is involved in regulating a myriad of physiological processes including, among many others, proliferation, differentiation, synaptic plasticity, and actions of hormones and neurotransmitters (2–4).

The homeostasis of cAMP is tightly controlled by the elaborate yet incompletely established network of players. cAMP is enzymatically synthesized from ATP by adenylyl cyclases (ACs) and degraded by phosphodiesterases. In mammals, there are nine transmembrane AC isoforms that show exquisite and differential regulation by a variety of mechanisms that include macromolecular scaffolding, binding of proteins and cofactors. Moreover, activity of ACs is also controlled by heavy metals (5, 6), calcium (7), and by a natural product forskolin, which acts through a distinct allosteric site (8, 9).

Perhaps the best characterized modulatory input into the AC system controlling cAMP dynamics is provided by G protein–coupled receptors (GPCRs), the largest family of cell surface receptors with prominent roles in cellular communication, physiology, and disease (10, 11). Most, if not all, canonical GPCRs signal by activating heterotrimeric G proteins, which entails their dissociation into Gα and Gβγ subunits. Most AC isoforms are activated by direct interaction with Gαs and Gαolf and are inhibited by binding to Gαi1, Gαi2, Gαi3, and Gαz (12, 13). In addition, ACs are regulated by the Gβγ subunits, which provide inhibition of some ACs while conditionally stimulating other isoforms (14). However, the mechanisms of AC regulation are not fully elucidated with a growing appreciation that there are a significant number of players with pivotal roles in cAMP regulation yet to be discovered.

Gβγ subunits have recently been identified to form a complex with members of the K^+ channel tetradimerization domain (KCTD) family of proteins (15, 16). KCTD oligomers have been identified as adapters that enable Cul3-mediated ubiquitin degradation of substrate proteins (17), including Gβγ dimers (16, 18). Interaction of certain KCTD members with Gβγ have also been shown to regulate Gβγ availability for engagement with some effectors (19–21). Although KCTD proteins have ties to GPCR signaling (15, 18), the action of KCTDs on cellular signaling and the mechanisms of their effects remain poorly understood. In this study, we report a previously unknown role of KCTD members in regulating AC with a major impact on neuronal cAMP dynamics and movement control in rodents.

Results

Loss of KCTD Proteins Selectively Impacts cAMP Production in Striatal Neurons. To study the role of KCTD proteins in the endogenous setting, we used a model of primary striatal neurons. Two distinct populations of neurons in the striatum process a variety of neuromodulatory signals programming responses related to movement coordination and reward valuation (22, 23). These signals converge on the cAMP system involving a well-characterized backbone of key elements (24–26), making it an attractive model for uncovering novel regulators of cAMP signaling (Fig. 1*A*). We implemented a CRISPR/Cas9 gene editing screen in primary striatal neurons from *cAMP Encoded Reporter* (*CAMPER*) mice, which conditionally express a cAMP biosensor (Fig. 1*B*) (27). A single-vector lentiviral system was used to unlock biosensor expression and to deliver both Cas9 nuclease and a single guide RNA (sgRNA)-targeting individual members of the KCTD family. In this system, three unique sgRNA targets were used for each gene (*SI Appendix*, Table S1). We chose to investigate KCTD proteins with ties to GPCR signaling, expanding the set to include homologous members of the subgroups: KCTD2, KCTD5, KCTD8, KCTD12, KCTD16, and

Significance

Neuromodulation is pivotal for brain function. One of the key pathways engaged by neuromodulators is signaling via second messenger cAMP, which controls a myriad of fundamental reactions. This study identifies KCTD5, a ubiquitin ligase adapter, as a regulatory element in this pathway and determines that it works by an unusual dual mode controlling the activity of cAMP-generating enzyme in neurons through both zinc transport and G protein signaling.

Author contributions: B.S.M. and K.A.M. designed research; B.S.M., S.M., X.L., and D.C.S. performed research; B.S.M., S.M., X.L., B.D.Y., J.A.W., and K.A.M. analyzed data; and B.S.M. and K.A.M. wrote the paper.

The authors declare no competing interest.

This article is a PNAS Direct Submission.

[1]To whom correspondence may be addressed. Email: bmuntean@augusta.edu or kirill@scripps.edu.

This article contains supporting information online at http://www.pnas.org/lookup/suppl/doi:10.1073/pnas.2119237119/-/DCSupplemental.

Published December 21, 2021.

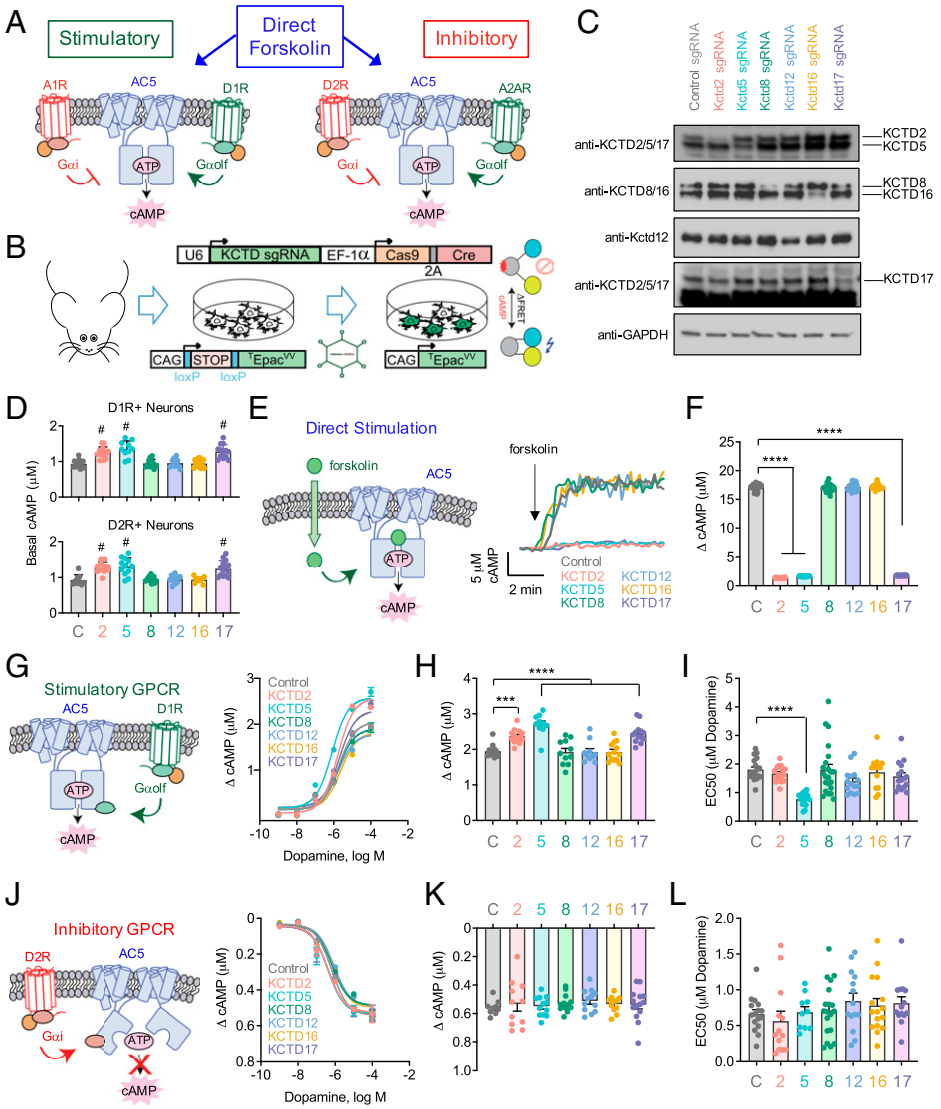

Fig. 1. KCTD proteins differentially regulate cAMP signaling in striatal neurons. (*A*) Scheme of inputs to AC5 in striatal medium spiny neurons. (*B*) CRISPR/Cas9 gene editing strategy in *CAMPER* primary striatal neurons. (*C*) Western blot for KCTD level in primary striatal neurons subject to CRISPR/Cas9 targeting of KCTDs or control. $n = 4$ cultures for each sgRNA. (*D*) Baseline cAMP values in D1R+ and D2R+ striatal neurons classified by directionality of response to dopamine. $n \geq 9$ neurons/group; one-way ANOVA; and #$P < 0.0001$. (*E*) Averaged cAMP responses to bath application of 100 μM forskolin. $n \geq 16$ neurons/group. (*F*) Max cAMP response amplitude to 100 μM forskolin in striatal neurons. $n \geq 16$ neurons/group; one-way ANOVA; and ****$P < 0.0001$. (*G*) Dopamine → D1R dose–response curve. $n \geq 13$ neurons/dose. (*H*) Max D1R response amplitude from 100 μM dopamine. $n \geq 10$ neurons/group; one-way ANOVA; ***$P < 0.001$; and ****$P < 0.0001$. (*I*) D1R response EC_{50} from dopamine. $n \geq 13$ neurons/dose; one-way ANOVA; and ****$P < 0.0001$. (*J*) Dopamine → D2R dose–response curve. $n \geq 9$ neurons/dose. (*K*) Max D2R response amplitude from 100 μM dopamine. $n \geq 9$ neurons/group. (*L*) D2R response EC_{50} from dopamine. $n \geq 9$ neurons/dose. All data represented as mean ± SEM.

KCTD17 (15, 16, 18). We first demonstrated in primary striatal neurons the lentiviral CRISPR strategy significantly lowered KCTD protein level of the targeted sgRNA with no effect on other KCTD members (Fig. 1*C* and *SI Appendix*, Fig. S1*A*). We then measured real-time cAMP dynamics in response to direct activation of AC with forskolin as well as to application of neurotransmitters dopamine and adenosine, which produce both stimulatory and inhibitory responses according to segregated GPCR expression in distinct populations of striatal neurons (Fig. 1*A*).

We first observed that elimination of some KCTDs (KCTD2, KCTD5, or KCTD17) but not others (KCTD8, KCTD12, or KCTD16) resulted in a significantly increased basal cAMP setpoint in both populations of striatal neurons (Fig. 1*D*). Application of forskolin produced rapid and robust increases in cAMP in all populations of striatal neurons (Fig. 1*E*). Strikingly, we observed that the response was virtually eliminated upon knockout of KCTD2, KCTD5, or KCTD17 (Fig. 1 *E* and *F*). In contrast deletion of other KCTD members (KCTD8, KCTD12, and KCTD16) had no influence on forskolin-mediated cAMP generation. These results indicate that several members of the KCTD family are required for setting cAMP tone as well as direct activation of AC by forskolin in striatal neurons.

To understand whether KCTDs affect cAMP production globally or have more selective effects we next evaluated the GPCR-driven responses. We first focused on stimulatory inputs to AC by recording cAMP responses initiated by the dopamine 1 receptor (D1R) in response to increasing dopamine concentrations (Fig. 1*G*). Remarkably, we observed that elimination of KCTD2, KCTD5, or KCTD17 enhanced cAMP production in

response to dopamine application as evidenced by the significantly larger response amplitudes with the effect of KCTD5 elimination being the greatest (Fig. 1*H*). Interestingly, elimination of KCTD5 also increased the sensitivity of responses to dopamine as evidenced by a leftward shift in the dose–response curve, significantly lowering the half maximal effective concentration (EC_{50}) values (Fig. 1*I*). No significant effects on either extent or sensitivity of dopamine-initiated cAMP production were observed upon elimination of KCTD8, KCTD12, or KCTD16.

To evaluate whether the observed effects were receptor specific, we also assessed stimulatory responses through the adenosine 2A receptor (A2AR) (*SI Appendix*, Fig. S1*B*). Similar to dopamine responses, we observed that elimination of KCTD5 increased both maximum response amplitude and potency (*SI Appendix*, Fig. S1*C*). Individual knockouts of all other KCTDs had no influence on response amplitude; however, loss of KCTD17 increased potency of adenosine responses (*SI Appendix*, Fig. S1*D*). A pattern emerged from the data whereby one group of KCTDs (KCTD2, KCTD5, and KCTD17) regulate cAMP production while the remaining group of KCTDs (KCTD8, KCTD12, or KCTD16) did not. Therefore, to evaluate functional redundancy of KCTD involvement, we next performed aggregate knock out for the members of each group at once and then assessed cAMP mobilization (*SI Appendix*, Fig. S1 *E–L*). We observed that simultaneous deletion of KCTD8/12/16 did not alter cAMP responses to both dopamine and adenosine, whereas aggregate KCTD2/5/17 knockout produced changes with similar effect size as loss of only KCTD5, suggesting that KCTD5 is the dominant regulator of cAMP responses in striatal neurons. To investigate whether results were due to off-target effects from our triple-sgRNA approach, we individually tested each of the three KCTD5 targeting sgRNAs. On their own, each sgRNA significantly reduced KCTD5 protein level (*SI Appendix*, Fig. S1*M*). Moreover, each individual KCTD5 sgRNA recapitulated the effects observed from pooled CRISPR approach on basal cAMP (*SI Appendix*, Fig. S1*N*), forskolin-mediated amplitude (*SI Appendix*, Fig. S1*O*), and responses to dopamine (*SI Appendix*, Fig. S1 *P* and *Q*). Overall, select KCTD members (KCTD2, KCTD5, and KCTD17) enhanced stimulatory AC inputs in nonredundant fashion with differential effects on response parameters, with no role in the process observed for KCTD8, KCTD12, or KCTD16.

Next, we assessed the contribution of KCTDs in regulating the inhibitory GPCR signaling to AC. We first confirmed identity of dopamine 2 receptor (D2R) containing primary striatal neurons with application of the D2R antagonist raclopride, which eliminated dopamine-mediated responses in D2R+ neurons but had no effect on D1R+ neurons (*SI Appendix*, Fig. S2 *A* and *B*). We then found that knockout of any KCTDs individually was unable to significantly alter either the potency or the efficacy of the cAMP suppressant effects mediated by the activation of D2R (Fig. 1 *J–L*). Similar lack of the effect was observed when the responses were triggered by the adenosine 1 receptor (A1R) (*SI Appendix*, Fig. S2 *C–E*). Simultaneous deletion of KCTD2/5/17 also failed to alter the properties of inhibitory responses to either dopamine or adenosine (*SI Appendix*, Fig. S2 *F–M*). In contrast, aggregate knockout of KCTD8/12/16 significantly diminished the maximal amplitudes of both A1R- and D2R-mediated responses without altering their potencies (*SI Appendix*, Fig. S2 *F–M*). We thus conclude that some KCTDs (KCTD8, KCTD12, and KCTD16) but not others (KCTD2, KCTD5, and KCTD17) redundantly regulate the efficacy of the inhibitory GPCR signaling to cAMP production.

Overall, our findings reveal that amid nuanced, largely negative impact on GPCR-mediated regulation of cAMP production, some KCTDs (KCTD2, KCTD5, and KCTD17) have striking permissive role of forskolin-mediated AC at the allosteric site with KCTD5 serving as a dominant player controlling all regulatory AC inputs in striatal neurons.

KCTD5 Controls cAMP Signaling through Zip14-Mediated Allosteric AC Regulation. The absolute requirement of select KCTDs for forskolin-mediated cAMP production is striking. Investigating the mechanisms of this regulation, we reasoned that because KCTDs have opposite inhibitory effect on GPCR-mediated stimulation, the effect on forskolin likely reflects altered allosteric regulation of AC. Indeed, forskolin binds to a presumptive allosteric pocket, distinct from the G protein–binding sites (8). Such allosteric sites on AC are heavily influenced by divalent metal ions (6, 7). Whereas Mg^{2+} or Mn^{2+} positively regulate AC activity, Zn^{2+} has been shown to potently suppress AC activity in reconstituted systems (5). To test a hypothesis regarding the involvement of Zn^{2+} in the effects of KCTDs, we first examined whether cAMP responses of striatal neuron to forskolin were sensitive to Zn^{2+}. Indeed, we observed that bath application of Zn^{2+} substantially diminished amplitudes of forskolin-mediated cAMP responses (Fig. 2 *A* and *B*). Curiously, mining the dataset of proteins targeted for degradation by the ubiquitin ligase activity of KCTD5 (18), we found metal transporter Slc39A14 (Zip14), with prominent role in the transport of Zn^{2+}, among the candidates. Validating this observation, we detected that knockout of KCTD5 as well as KCTD2 and KCTD17 resulted in approximately twofold increase in Zip14 levels (Fig. 2*C*). To further investigate, we examined Zip14 ubiquitination by KCTD5 in transfected human embryonic kidney 293 (HEK 293) cells. The Zip14 degradation process has been previously reported (28) and consists of deglycosylation (Zip14-DG) and ubiquitination (Zip14-Ub), resulting in both lower (Zip14-DG)– and higher (Zip14-Ub)–molecular weight forms. Incubation with the proteasome inhibitor Bortezomib resulted in the accumulation of both Zip14-DG and Zip14-Ub upon overexpression of ubiquitin machinery (Ubiquitin, Cul3, and NEDD8) but not in Zip14 transfection alone (Fig. 2*D*). Strikingly, cotransfection of Zip14 with KCTD5 alone also induced the emergence of Zip14-DG and Zip14-Ub, suggesting that increasing the abundance of KCTD5 is sufficient to induce Zip14 ubiquitination and subsequent degradation. This finding indicates that Zip14 is indeed targeted for degradation by KCTD5, suggesting that elevation of Zip14 levels in striatal neurons lacking KCTD5 may be mechanistically explained by inhibition of Zip14 degradation.

To examine the consequence of increased Zip14, we studied its role in Zn^{2+} transport into striatal neurons using the fluorescent zinc biosensor Fluozin-3 (Fig. 2*E*). Bath application of Zn^{2+} at a physiologically relevant 1 μM concentration (29) resulted in a slow Zn^{2+} entry (Fig. 2*F*). The rate of the Zn^{2+} flux was substantially accelerated by Zip14 overexpression, consistent with its role in intracellular Zn^{2+} transport. Remarkably, we found that KCTD5 elimination resulted in a comparable increase in Zn^{2+} transport (Fig. 2*F*). Importantly, dose–response studies revealed that Zip14 overexpression and KCTD5 elimination both caused similar leftward shifts allowing loading the neurons at much-lower extracellular Zn^{2+} concentrations as compared with control neurons (Fig. 2 *G* and *H*). Furthermore, both Zip14 overexpression and KCTD5 elimination produced significant increases in the maximum amount of Zn^{2+} loaded into the neurons, allowing higher intracellular concentrations to be achieved (Fig. 2*I*).

To determine the causal connection between KCTD5 and Zip14 in regulating AC activity, we performed a genetic epistasis experiments in *CAMPER* neurons (Fig. 2*J*). First, we verified that overexpression of Zip14 was sufficient to occlude forskolin-mediated cAMP responses (Fig. 2*K*). Given their opposing presumptive relationship, we argued that if KCTD5 effects on forskolin-stimulated cAMP generation are solely

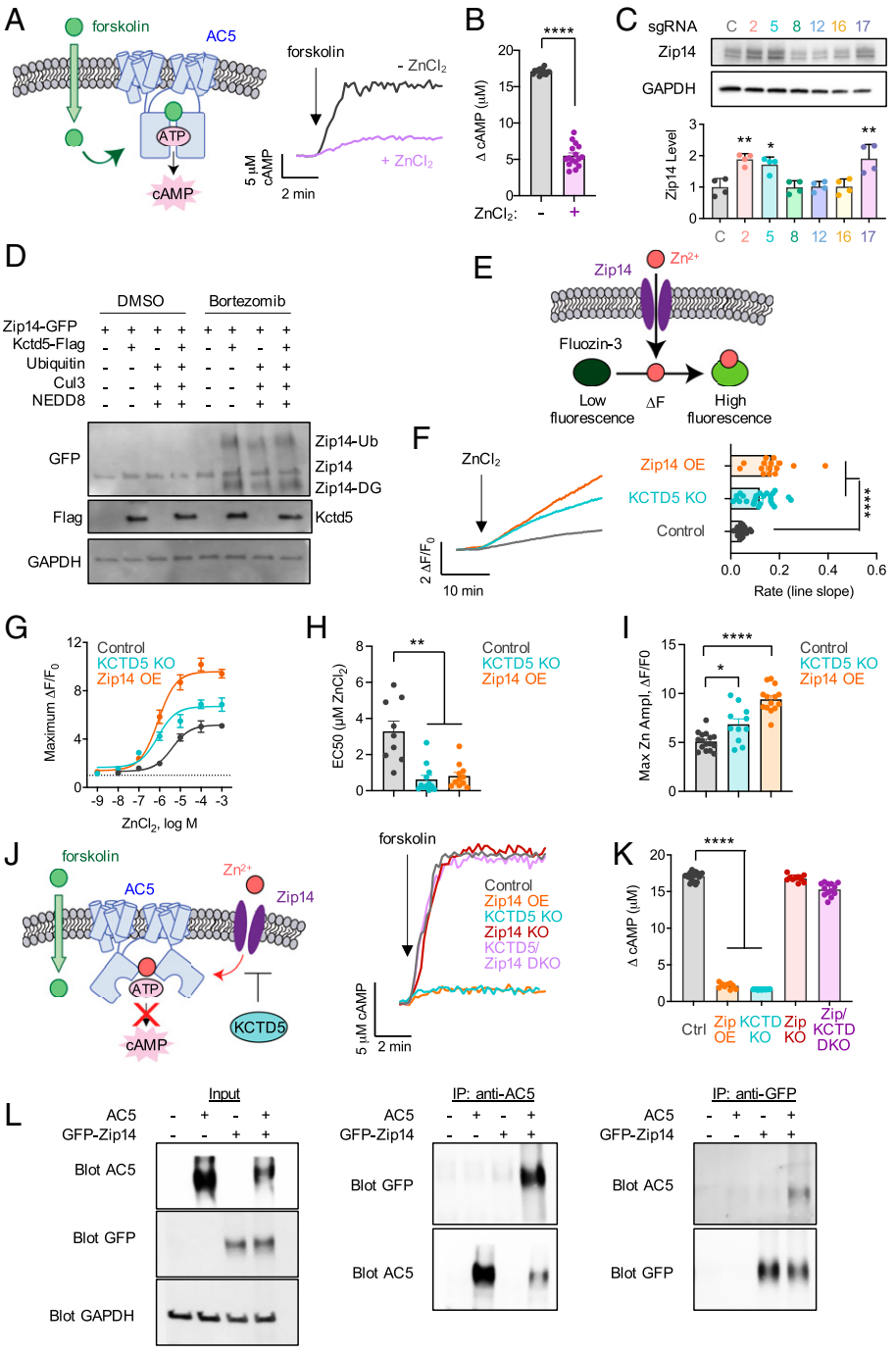

Fig. 2. KCTD5 modulates AC5 activity through Zip14-mediated zinc flux. (*A*) Averaged cAMP responses to bath application of 100 µM forskolin in striatal neurons in the presence or absence of zinc chloride (100 µM). $n = 16$ neurons/group. (*B*) Max cAMP response amplitude to 100 µM forskolin in the presence or absence of zinc chloride (100 µM). $n = 16$ neurons/group; nonparametric Mann–Whitney *U* test; and $^{****}P < 0.0001$. (*C*) Western blot for Zip14 level in primary striatal neurons subject to CRISPR/Cas9 targeting of KCTDs or control. $n = 4$ cultures/group; one-way ANOVA Tukey comparison test to control sgRNA; $^{*}P < 0.05$; and $^{**}P < 0.01$. (*D*) Western blot from HEK293 cells with indicated transfection and 2-h treatment with dimethyl sulfoxide (DMSO) or Bortezomib (100 nM). Bands labeled for ubiquitinated Zip14-Ub and Zip14-DG. Representative blot of three independent experiments. (*E*) Scheme of Fluozin-3 sensor responding to Zn^{2+}. (*F*) Averaged Zn2+ responses to bath application of 1 µM zinc chloride in striatal neurons ($n = 27$ control CRISPR/Cas9, $n = 25$ KCTD5 CRISPR/Cas9 knockout, and $n = 15$ Zip14 overexpression) and rate of Zn2+ flux in striatal neurons. $n = 27$ control CRISPR/Cas9 ($r^2 = 0.969$), $n = 25$ KCTD5 CRISPR/Cas9 knockout ($r^2 = 0.967$), $n = 15$ Zip14 overexpression ($r^2 = 0.979$); one-way ANOVA Dunnett's multiple comparison; and $^{****}P < 0.0001$. (*G*) Zinc flux dose–response curve. $n \geq 9$ neurons/dose. (*H*) Zinc flux EC_{50}. $n \geq 9$ neurons/dose; one-way ANOVA Dunnett's multiple comparison; and $^{**}P < 0.01$. (*I*) Max zinc flux. $n \geq 11$neurons/group; one-way ANOVA Dunnett's multiple comparison; $^{*}P < 0.05$, and $^{****}P < 0.0001$. (*J*) Averaged cAMP responses to bath application of 100 µM forskolin. $n \geq 9$ neurons/group. (*K*) Max cAMP response amplitude to 100 µM forskolin in striatal neurons. $n \geq 9$ neurons/group; one-way ANOVA Dunnett's multiple comparison; and $^{****}P < 0.0001$. (*L*) AC5 and Zip14 coimmunoprecipitate in transfected HEK293T/17 cells. Representative data from three independent experiments. All data represented as mean ± SEM.

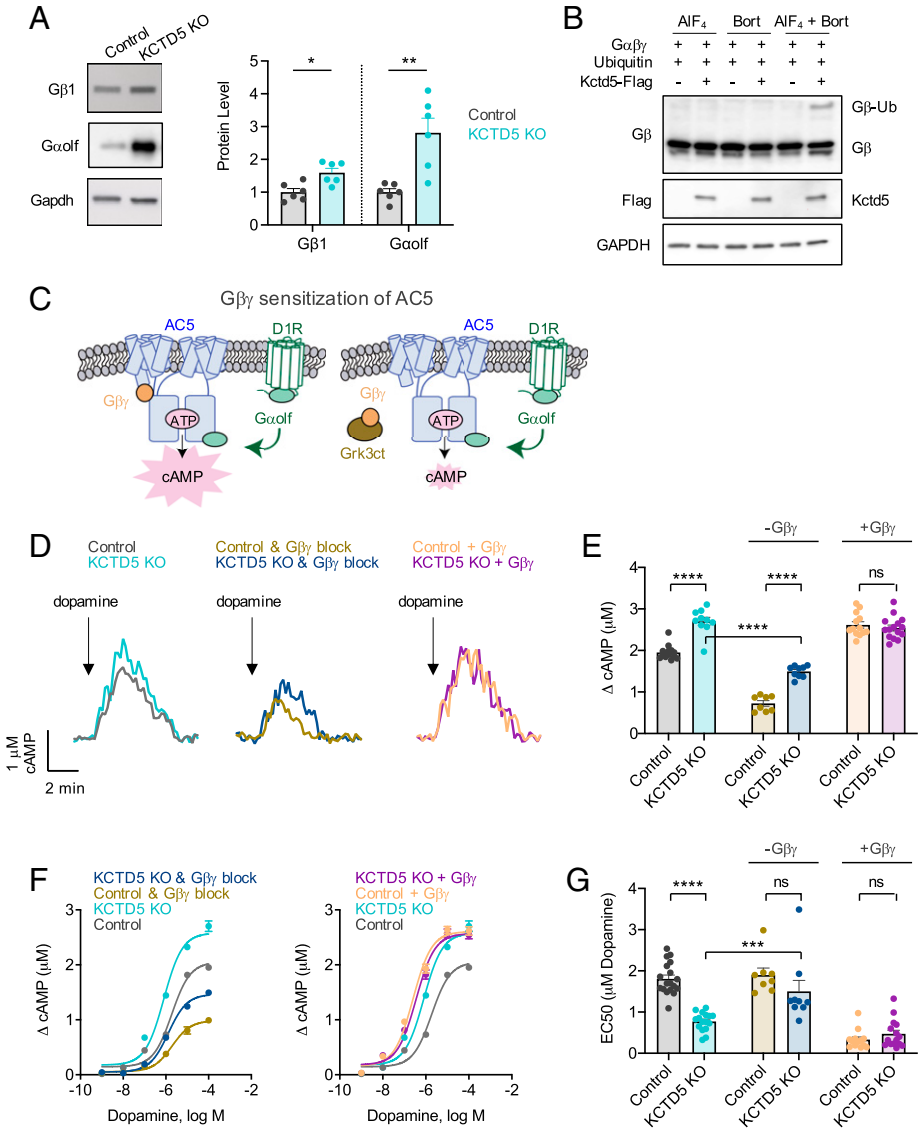

Fig. 3. KCTD5 sensitizes striatal cAMP signaling through Gβγ regulation. (*A*) Western blot analysis from cultured striatal neurons subject to CRISPR/Cas9 targeting of either KCTD5 or scrambled control. $n = 6$ cultures/group; nonparametric Mann–Whitney *U* test; $^{*}P < 0.05$; and $^{**}P < 0.01$. (*B*) Western blot from HEK293 cell with indicated transfection (Gαo, Gβ2, Gγ7, ubiquitin, and KCTD5) and 2-h treatment with AlF_4 (30 μM), Bortezomib (100 nM), or both. Band labeled for ubiquitinated Gβ (Gβ-Ub). Representative blot of three independent experiments. (*C*) Gβγ-mediated sensitization of Gαolf-AC-cAMP signaling is attenuated by the Gβγ-scavenger Grk3ct. (*D*) Representative D1R-mediated cAMP responses to a phasic puff of 100 μM dopamine (*Left*), with Grk3ct overexpression (Gβγ block; *Middle*) or Gβγ overexpression (+Gβγ; *Right*). $n \geq 8$ neurons/group. (*E*) Max D1R response amplitude from 100 μM dopamine. $n \geq 8$ neurons/group; nonparametric Mann–Whitney *U* test; and $^{****}P < 0.0001$. (*F*) Dopamine → D1R dose–response curve with Grk3ct overexpression (Gβγ block; *Left*) or Gβγ overexpression (+Gβγ; *Right*). $n \geq 8$ neurons/dose. (*G*) D1R response EC_{50} from dopamine. $n \geq 14$ neurons/dose; nonparametric Mann–Whitney *U* test; ns $P > 0.05$; $^{***}P < 0.001$; and $^{****}P < 0.0001$. All data represented as mean ± SEM.

mediated by Zip14, we should be able to rescue the loss of responsiveness phenotype in KCTD5 knockout neurons by additional elimination of Zip14. Indeed, while knockout of Zip14 alone did not alter cAMP generation kinetics, Zip14 elimination in neurons lacking KCTD5 restored responses to forskolin back to profile observed in control neurons (Fig. 2*K*).

The extreme sensitivity of cAMP regulation to Zn^{2+} in striatal neurons, despite expectedly high level of metal ion buffering by cytoplasmic metalloproteins (30), prompted us to explore a possibility that Zip14 could be macromolecularly integrated with the cAMP-producing machinery. We examined the interaction between Zip14 and dominant striatal AC isoform, AC type 5 (AC5), transfected into HEK293 cells. We detected a robust coimmunoprecipitation of AC5 with Zip14 in both forward and the reverse directions upon their coexpression (Fig. 2*L*). Skipping the antibody target in the control experiments showed that this interaction was specific. Collectively, these results indicate that in striatal neurons, KCTD5 acts as a major regulator of cAMP production, acting to regulate Zn^{2+} homeostasis by controlling the level of Zip14 transporter, which in turn forms macromolecular complexes with AC5 delivering Zn^{2+} ions for the allosteric control of the enzyme.

KCTD5 Regulates Stimulatory GPCR Inputs to AC through Gβγ. We next turned to resolve the mechanisms by which KCTD5 inhibits its GPCR-driven responses. Because this regulation was opposite from the Zip14/Zn^{2+}-mediated regulation of allosteric site, we reasoned that it involves a distinct molecular entity. An attractive candidate for mediating GPCR effects of KCTD5 is Gβγ. It is known to exert a stimulatory effect on striatal AC5

(31) and has also been recently identified as a ubiquitination substrate of KCTD5 (16, 18). We therefore hypothesized that elimination of KCTD5 could enhance Gβγ stability, resulting in increased availability, enabling sensitization of AC activity. Analysis of protein levels in primary cultured striatal neurons revealed that KCTD5 elimination caused a significant up-regulation of $G\beta_1$, an abundant component (26) of Gβγ complexes in the stratum (Fig. 3*A*). Moreover, KCTD5 deletion similarly increased levels of Gαolf (Fig. 3*A*). Next, we transfected HEK293 cells with G protein heterotrimer with or

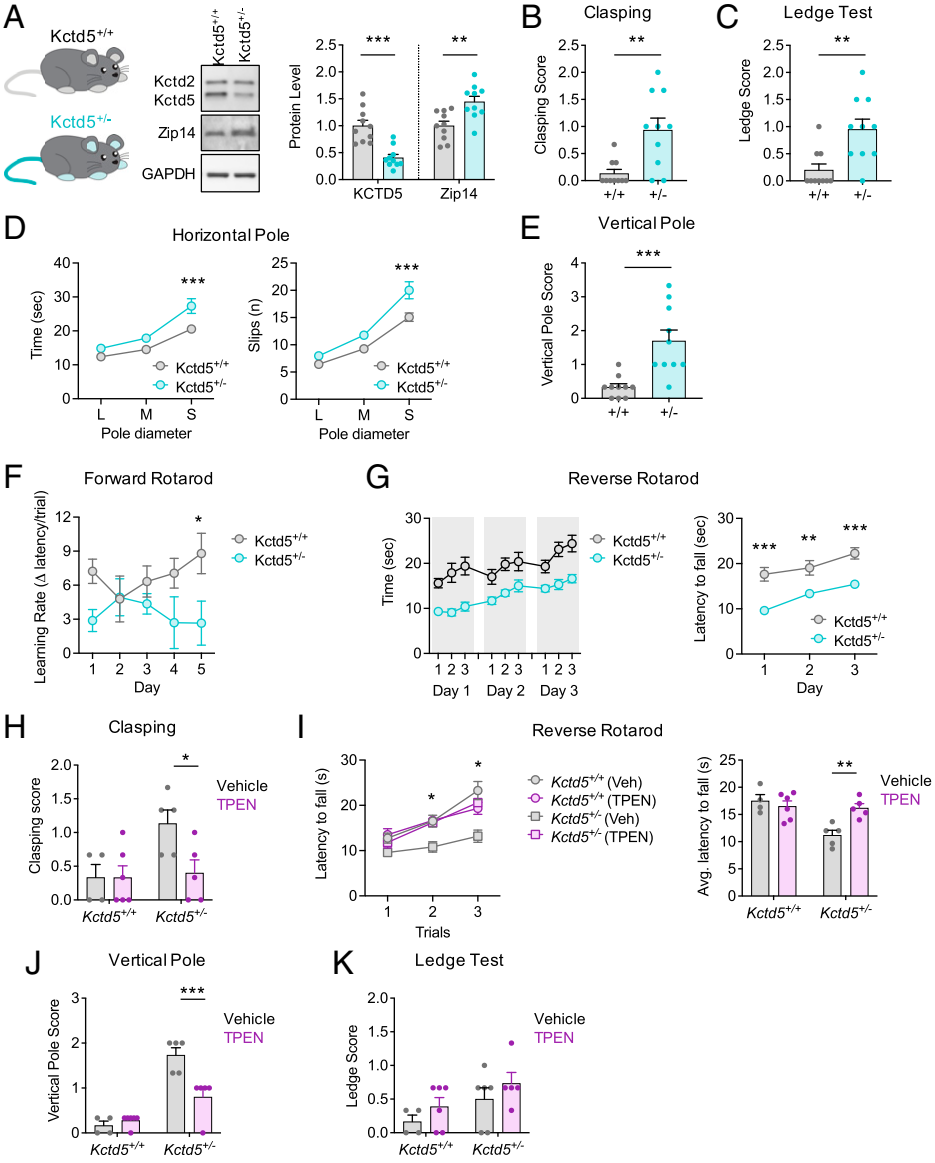

Fig. 4. KCTD5 haploinsufficiency drives motor impairments in mice. A total of 20 mice in two groups of *Kctd5* mice (i.e., wild-type [$Kctd5^{+/+}$], $n = 6$ [male] and 4 [female], and heterozygous [$Kctd5^{+/-}$], $n = 5$ [male] and 5 [female]) were used for behavioral analysis. (*A*) Western blot from dorsal striatal tissue punches taken from $Kctd5^{+/+}$ and $Kctd5^{+/-}$. $n = 10$ mice per group; nonparametric Mann–Whitney *U* test; $^{**}P = 0.0052$; and $^{***}P = 0.0002$. (*B*) Hindlimb-clasping pathology score for $Kctd5^{+/+}$ ($n = 10$) and $Kctd5^{+/-}$ ($n = 10$) mice (unpaired *t* test; parametric; and $^{**}P = 0.003$). (*C*) Ledge test pathology score for $Kctd5^{+/+}$ ($n = 10$) and $Kctd5^{+/-}$ ($n = 10$) mice (unpaired *t* test; parametric; and $^{**}P = 0.003$). (*D*) Horizontal pole test for $Kctd5^{+/+}$ ($n = 10$) and $Kctd5^{+/-}$ ($n = 10$) mice with varying pole diameter: 15.8 (L), 11 (M), and 8 (S) mm (*Left*). Time to complete test is shown (two-way ANOVA; Sidak multiple comparison test; and $^{***}P < 0.001$) (*Right*). Number of hindlimb slips during test (two-way ANOVA; Sidak multiple comparison test; and $^{***}P < 0.001$). (*E*) Vertical pole test score for $Kctd5^{+/+}$ ($n = 10$) and $Kctd5^{+/-}$ ($n = 10$) mice (unpaired *t* test; parametric; and $^{***}P < 0.001$). (*F*) Learning rate on accelerating rotarod for $Kctd5^{+/+}$ ($n = 10$) and $Kctd5^{+/-}$ ($n = 10$) mice. (Two-way ANOVA; Sidak multiple comparison test; and $^{*}P = 0.038$). (*G*) Latency to fall while walking backward on a rotating beam for $Kctd5^{+/+}$ ($n = 10$) and $Kctd5^{+/-}$ ($n = 10$) mice (*Left*). Three intraday trials over 3 d are shown (*Right*). Average of daily latency (two-way ANOVA; Sidak multiple comparison test; $^{**}P = 0.003$, and $^{***}P < 0.001$). (*H*) Hindlimb-clasping pathology score for mice treated with vehicle ($Kctd5^{+/+}$ $n = 4$, $Kctd5^{+/-}$ $n = 5$) or TPEN ($Kctd5^{+/+}$ $n = 6$, $Kctd5^{+/-}$ $n = 5$). Two-way ANOVA; Sidak multiple comparison test; and $^{*}P = 0.0295$. (*I*) Latency to fall while walking backward on a rotating beam for mice treated with vehicle ($Kctd5^{+/+}$ $n = 4$, $Kctd5^{+/-}$ $n = 5$) or TPEN ($Kctd5^{+/+}$ $n = 6$, $Kctd5^{+/-}$ $n = 5$) (*Left*). Average from interday trials; two-way repeated measures (RM) ANOVA; Tukey multiple comparison test; and $^{*}P < 0.05$ for $Kctd5^{+/-}$ (TPEN) versus other groups (*Right*). Average latency from all trials; two-way ANOVA; Sidak multiple comparison test; and $^{**}P = 0.004$. (*J*) Vertical pole test score for mice treated with vehicle ($Kctd5^{+/+}$ $n = 4$, $Kctd5^{+/-}$ $n = 5$) or TPEN ($Kctd5^{+/+}$ $n = 6$, $Kctd5^{+/-}$ $n = 5$). Two-way ANOVA; Sidak multiple comparison test; and $^{***}P = 0.0004$. (*K*) Ledge test pathology score for mice treated with vehicle ($Kctd5^{+/+}$ $n = 4$, $Kctd5^{+/-}$ $n = 5$) or TPEN ($Kctd5^{+/+}$ $n = 6$, $Kctd5^{+/-}$ $n = 5$). Two-way ANOVA; Sidak multiple comparison test. All data represented as mean ± SEM.

without KCTD5. Dissociation of Gβγ from the complex with AlF_4 resulted in the appearance of prominent monoubiquitinated Gβ band (Gβ-Ub) upon proteasome blockade only when KCTD5 was present (Fig. 3*B*). The observation indicates that the heterotrimeric G protein complexes are indeed regulated by KCTD5, leading to direct ubiquitin-mediated degradation of Gβ, which in turn destabilizes associated Gα. Finally, we found that Gβ levels are similarly up-regulated in striatal neurons upon knockout of KCTD2 and KCTD17 but not KCTD8, KCTD12, or KCTD16 (*SI Appendix*, Fig. S3*A*).

To test whether the enhancement of cAMP responses to stimulatory GPCR activation could be indeed explained by excess Gβγ, we performed both loss and gain of function experiments (Fig. 3*C*). First, we blocked Gβγ–AC5 interaction by overexpressing the Gβγ scavenger GRK3CT, known to prevent Gβγ binding to effectors (32). We found that Gβγ blockade indeed abolished the effects of KCTD5 elimination (Fig. 3*D* and *SI Appendix*, Fig. S3*B*) through a reduction in maximum cAMP efficacy (Fig. 3*E* and *SI Appendix*, Fig. S3*C*). While Gβγ blockade did not have a significant effect on the sensitivity of the control neurons' responses to dopamine (Fig. 3*F*) and adenosine (*SI Appendix*, Fig. S3*D*), mediated by D1R and A2R respectively, GRK3CT increased EC_{50} values for both neurotransmitters in KCTD5 knockout neurons back to their wild-type levels (Fig. 3*G* and *SI Appendix*, Fig. S3*E*).

We next overexpressed the Gβγ dimer aiming to saturate its sensitizing effect on AC5 and thereby bypass the action of KCTD5 if the effect of its elimination is indeed due to the increased Gβγ availability. Consistent with the published literature, we found that overexpression of Gβγ in control neurons increased the sensitivity of dopamine and adenosine responses as well as augmented their maximal amplitudes (Fig. 3 *D–G* and *SI Appendix*, Fig. S3 *B–E*). This effect essentially phenocopied the behavior of KCTD5 knockout neurons. Importantly, Gβγ overexpression failed to significantly alter response properties of both transmitters in the absence of KCTD5, suggesting that Gβγ overexpression and KCTD5 loss work through the same mechanism. Collectively, this data indicates that KCTD5 tunes GPCR signaling to cAMP production by regulating the extent of Gβγ available for AC binding.

KCTD5 Regulates Animal Motor Behavior in a Zn^{2+}-Dependent Manner. Our data thus far collectively demonstrate a role for KCTD5 in regulating striatal cAMP through a combination of mechanisms. Because disruption of the striatal cAMP system is often associated with impairments in control of movements (33), we next investigated the role of KCTD5 in regulating motor control in vivo. Breeding mice with a null *Kctd5* allele did not produce any homozygous littermates, suggesting embryonic lethality upon complete elimination of KCTD5. However, heterozygous $Kctd5^{+/-}$ mice were viable and appeared normal. We found that KCTD5 levels were significantly reduced in the dorsal striatum of these mice, revealing KCTD5 haploinsufficiency (Fig. 4*A*). Moreover, Zip14 level was significantly up-regulated in the striatal tissues of $Kctd5^{+/-}$ mice (Fig. 4*A*).

To assess behavioral implications of KCTD5 reduction, we employed a panel of assays for motor behaviors sensitive to perturbations in the striatal circuitry (34). We found that $Kctd5^{+/-}$ mice showed significant hindlimb-clasping phenotype, a hallmark dystonic feature absent in wild-type ($Kctd5^{+/+}$) (Fig. 4*B*). The $Kctd5^{+/-}$ mice also performed consistently worse than $Kctd5^{+/+}$ littermates in behavioral tests designed to test limb coordination: ledge walking (Fig. 4*C*), horizontal (Fig. 4*D*), and vertical (Fig. 4*E*) pole tests. Next, we assessed motor skill learning and consolidation by evaluating mice on an accelerating rotarod over 5 consecutive d with 10 intraday trials (*SI Appendix*, Fig. S4*A*). This test revealed that $Kctd5^{+/-}$ mice had significantly reduced improvements in motor learning compared with $Kctd5^{+/+}$

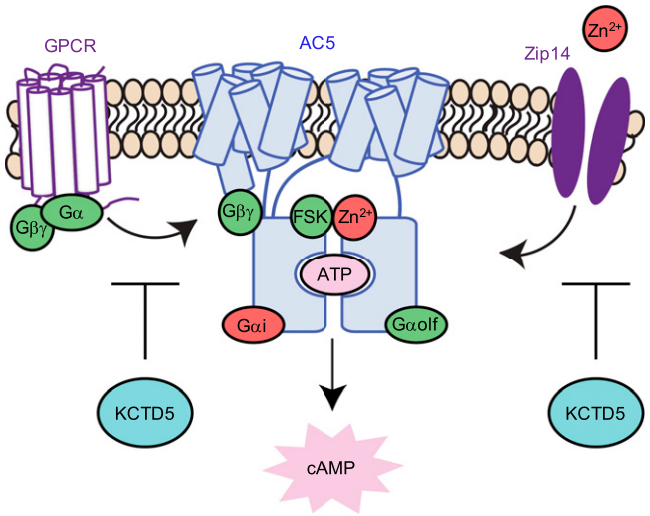

Fig. 5. Dual modulation of AC5 activity by KCTD mediated through Gβγ and Zip14. Schematic illustration of distinct binding domains on AC5. Occupation of binding sites enable substrates to modulate degree of open (active) and closed (inactive) conformation state of the enzyme, subsequently altering catalytic activity. Green substrates favor open (active) state, and red substrates favor closed (inactive) state. Gβγ binds intracellular N terminus. Gαi and Gαolf have distinct binding site on catalytic domains (C1 and C2, respectively). Forskolin (FSK) and Zn^{2+} bind near ATP. In our model, Zip14 proximity facilitates loading Zn^{2+} in AC5. KCTD5 inhibits both Gβγ and Zip14, thus exerting dual regulation over AC5 activity.

littermates (Fig. 4*F*). These deficits were more pronounced upon increasing the challenge in the test by reversing the rotation direction so that the animals walk backward (Fig. 4*G*).

We next assessed whether motor deficits were due to irregularities in ambulatory ability or generalized behavioral deficits. We first found that all animals had similar grip strength (*SI Appendix*, Fig. S4*B*). We next evaluated mice in the open-field test (*SI Appendix*, Fig. S4 *C–J*). No statistical differences were observed between genotype or sex in any of the parameters: distance traveled (*SI Appendix*, Fig. S4 *C* and *D*), velocity (*SI Appendix*, Fig. S4 *E* and *F*), time spent in center (*SI Appendix*, Fig. S4 *G* and *H*), and time spent in corner (*SI Appendix*, Fig. S4 *I* and *J*).

To test whether an excess of zinc generated by up-regulation of Zip14 upon KCTD5 loss may play a role in motor deficits observed in Kctd5 haploinsufficient mice, we treated mice chronically with a Zn^{2+} ion chelator N, N, N', N-Tetrakis (2-pyridylmethyl) ethylenediamine (TPEN). Strikingly, TPEN treatment completely rescued the hindlimb-clasping (Fig. 4*H*) as well as the limb coordination in the backward-walking assay (Fig. 4*I*) in $Kctd5^{+/-}$ mice. TPEN treatment also partially rescued the $Kctd5^{+/-}$ deficits observed in the vertical pole assay (Fig. 4*J*) but had no effect on animal behavior in the ledge test (Fig. 4*K*). These effects were specific, as control $Kctd5^{+/+}$ animals were not influenced by the TPEN treatment.

Overall, our behavioral experiments reveal that KCTD5 haploinsufficiency in mice significantly compromises motor behavior which could be partially rescued by zinc chelation, providing in vivo evidence for KCTD5 in controlling GPCR-signaling pathways via Zn^{2+} dependent mechanisms.

Discussion

In this study, we link enigmatic members of KCTD family to regulation of a key cellular second messenger system—the cAMP pathway. The KCTD proteins were originally identified for their role in regulating kinetics and magnitude of $GABA_B$ receptor singling to G protein inwardly rectifying K^+ (15, 19).

PHARMACOLOGY

It has been subsequently determined that they do so by specific and direct interaction with both $GABA_B$ and Gβγ acting as scaffolds (20, 21, 35). Furthermore, some KCTDs have been also found to serve as adaptors for cullin 3 ubiquitin ligases (36), and Gβγ has been identified as one of their targets (16, 18). The current study expands these isolated reports to reveal that KCTDs are generally involved in regulating GPCR signaling via effects on the cAMP system.

Our systematic profiling of KCTD family in the endogenous setting of native striatal neurons identified that a major role in defining GPCR signaling to cAMP belongs to KCTD5 (Fig. 5). We identified that KCTD5 acts by a two-tiered mechanism to exert its effects. First, we show that KCTD5 acts to regulate stimulation of AC by Gαs/Gαolf adjusting potency and efficacy of GPCR inputs in a Gβγ-dependent manner. These effects are consistent with the identified role of KCTD5 as a ubiquitin ligase for Gβγ (16, 18) and are thus likely brought about by direct regulation of Gβγ stability by KCTD5. The second mechanism is intriguing, unexpected, and sheds light onto neuromodulatory system that adjusts neuronal responses. We found that KCTD5 is a powerful modulator for the Zn^{2+} effects on GPCR signaling, acting via controlling the expression of Zip14, a metal transporter that regulates Zn^{2+} flux. We found that loss of KCTD5 leads to increased zinc influx, which in turn reduces efficacy at the allosteric binding site on AC. The extent of this effect is striking: knockout of KCTD5 essentially abolished cAMP accumulation in response to forskolin. Prior studies support the role of Zip14 in regulation of cAMP (37); however, we offer a mechanistically distinct explanation of the reactions underlying this regulation.

Our observations uncover a fundamental role of Zn^{2+} in regulation of striatal GPCR inputs, outside of the described role for zinc in contributing to neuronal activity and circuitry. In general, glutamatergic neurons pack labile zinc into synaptic vesicles with glutamate (38). Neurotransmitter corelease enables Zn^{2+} to allosterically modulate synaptic plasticity by inhibition of key postsynaptic players including NMDAR (39) and $GABA_A$ (40). Particularly in the striatum, zinc modulation of ion channels tunes electrical activity (41–43) and inhibits excitatory responses from endogenous inputs (44). Given the key cAMP-mediated role in regulating both NMDAR (45) and $GABA_A$ (46), electrical conductance is likely further influenced by the mechanism we report here by which Zip14 tunes GPCR responses in striatal neurons by modulating zinc homeostasis and zinc entry into neurons. We found a major target of Zn^{2+} in striatal neurons is regulation by Zip14–AC5, placing AC5 on a growing list of molecules (e.g., PKC, PLC, TRPV, and TRPM7) influenced by zinc transients (47). Although metal-binding sites in AC5 are thought to be canonically occupied by Mg^{2+}, structures of the enzyme bound to Zn^{2+} have been solved (6). We propose a model in which Zip14–AC5 proximity facilitate Zn^{2+} displacement of Mg^{2+}. Indeed, Zn^{2+}-binding induces conformational changes in AC5 (48) thought to facilitate enzymatic inhibition (5). Consistent with this model are further observations in the hippocampus where Zn^{2+} has been shown to attenuate forskolin-induced LTP (49), which occurs in the concentration range of synaptically released Zn^{2+} (50). This mechanism may be generalized across the brain, perhaps incorporating tissue specificity of Zip family members, given that most ACs are regulated by forskolin.

We think that several KCTD proteins likely share common mechanisms by which they regulate cellular signaling. All KCTD proteins contain N-terminal BTB domains that mediate protein interactions, which include binding partners such as $GABA_B$ receptor, Cul3, and Gβγ (20, 21, 36). Intriguingly, KCTDs also homo-oligomerize into tetramers and pentamers, which is thought to enhance affinity with binding partners (36, 51, 52). It has recently been demonstrated that KCT12 and KCTD16 form functional heter-oligomeric complexes (53). In principle, hetero complex assembly is plausible across the KCTD subfamilies that share homology and likely organizes higher-level complexity of KCTD regulation over GPCR signaling. For example, in regulation of inhibitory G protein inputs to AC, we observed redundancy in the roles between KCTD8, KCTD12, and KCDT16. Elimination of all three of these KCTDs was therefore necessary to compromise reduction of cAMP formation upon activation of inhibitory GPCRs. It is tempting to speculate that the more prominent effects of KCTD5 over other members in regulating stimulatory G protein signaling may be explained by its ability to endow KCTD heteromers with high-affinity Gβγ recognition in which even subtle change in Gβγ concentration exerts significant impact on adjusting stimulatory inputs to AC.

Finally, it is interesting to consider implications of the identified KCTD-mediated regulation of cAMP signaling for understanding pathophysiological process. KCTD-associated impairments include movement disorder (KCTD17) (54), autism spectrum disorder (KCTD13 and KCTD21) (55, 56), bipolar disorder (KCTD12) (57), epilepsy (KCTD3 and KCTD7) (58, 59), and Alzheimer's disease risk (KCTD2) (60). We believe that the implication of numerous KCTDs in diverse pathologies highlights the potential for the entire KCTD family to serve as neuromodulatory adjustors of GPCR–cAMP signaling, depending on cell type–specific KCTD contributions in driving neural networks. We demonstrate how this process is further nuanced in the case of KCTD5-mediated regulation of Zip14. Interestingly, haploinsufficiency in mice resulted in significant motor impairments, which were improved by zinc chelation therapy. Restoration of many but not all behavioral deficits may be due to the dichotomous role of KCTD5 in regulating both G protein and Zip14-mediated activity of cAMP dynamics, in which some behaviors may be more sensitive to modulation by Zn^{2+} signaling. In alignment with our behavioral observation, clinical variants in the Zip14-encoding gene, Slc39a14, have recently been implicated in parkinsonism–dystonia (61). This connects KCTDs and Zip14 to a series of striatal cAMP regulators causal to movement disorders that includes AC5 (62), Gαolf (63), Gαo (34, 64, 65), Gβ1 (66, 67), and PDE10A (68). The diversity of KCTD interactome, defined in part by their cooperative hetero-oligomeric complex assembly, introduces a distinct signaling paradigm to our understanding of cAMP regulation. We are hopeful that future investigation will unravel further signaling logistics and components in striatal GPCR pharmacology repertoire.

Materials and Methods

All animal experiments were conducted in accordance with the Guide for the Care and Use of Laboratory Animals of the NIH and approved by the Institutional Animal Care and Use Committee at The Scripps Research Institute. Animal studies involved the use of mouse reporter strain CAMPER to study the dynamics of cAMP by imaging cultures of striatal neurons and Kctd5 knockout mice used for behavioral evaluation. Standard confocal imaging methods were applied. Animal behavior was assessed in a panel of assays evaluating motor performance. We used previously published methods for primary neuronal cultures and CRISPR/Cas9 genetic manipulations. Protein–protein interactions were studied by immunoprecipitation, and protein ubiquitination was analyzed by Western blotting. Comprehensive details for behavioral experiments, neuronal imaging studies, in vitro assays, and statistical analysis are provided in *SI Appendix, SI Materials and Methods*.

Data Availability. All study data are included in the article and/or *SI Appendix*.

ACKNOWLEDGMENTS. We thank Natalia Martemyanova for husbandry, maintenance, and genotyping of the mice used in this study. This work was supported by NIH Grant DA036596 (K.A.M.), Department of Defense Award W81XWH-19-1-0063, and funding from Augusta University (B.S.M.).

1. J. A. Beavo, L. L. Brunton, Cyclic nucleotide research – Still expanding after half a century. *Nat. Rev. Mol. Cell Biol.* **3**, 710–718 (2002).
2. S. R. Post, H. K. Hammond, P. A. Insel, Beta-adrenergic receptors and receptor signaling in heart failure. *Annu. Rev. Pharmacol. Toxicol.* **39**, 343–360 (1999).
3. E. R. Kandel, The molecular biology of memory storage: A dialogue between genes and synapses. *Science* **294**, 1030–1038 (2001).
4. R. L. Davis, J. Cherry, B. Dauwalder, P. L. Han, E. Skoulakis, The cyclic AMP system and Drosophila learning. *Mol. Cell. Biochem.* **149-150**, 271–278 (1995).
5. C. Klein, R. K. Sunahara, T. Y. Hudson, T. Heyduk, A. C. Howlett, Zinc inhibition of cAMP signaling. *J. Biol. Chem.* **277**, 11859–11865 (2002).
6. J. J. Tesmer *et al.*, Two-metal-Ion catalysis in adenylyl cyclase. *Science* **285**, 756–760 (1999).
7. B. Hu, H. Nakata, C. Gu, T. De Beer, D. M. Cooper, A critical interplay between Ca2+ inhibition and activation by Mg2+ of AC5 revealed by mutants and chimeric constructs. *J. Biol. Chem.* **277**, 33139–33147 (2002).
8. J. J. Tesmer, R. K. Sunahara, A. G. Gilman, S. R. Sprang, Crystal structure of the catalytic domains of adenylyl cyclase in a complex with Gsalpha.GTPgammaS. *Science* **278**, 1907–1916 (1997).
9. K. B. Seamon, W. Padgett, J. W. Daly, Forskolin: Unique diterpene activator of adenylate cyclase in membranes and in intact cells. *Proc. Natl. Acad. Sci. U.S.A.* **78**, 3363–3367 (1981).
10. K. L. Pierce, R. T. Premont, R. J. Lefkowitz, Seven-transmembrane receptors. *Nat. Rev. Mol. Cell Biol.* **3**, 639–650 (2002).
11. N. Wettschureck, S. Offermanns, Mammalian G proteins and their cell type specific functions. *Physiol. Rev.* **85**, 1159–1204 (2005).
12. R. Sadana, C. W. Dessauer, Physiological roles for G protein-regulated adenylyl cyclase isoforms: Insights from knockout and overexpression studies. *Neurosignals* **17**, 5–22 (2009).
13. R. K. Sunahara, C. W. Dessauer, A. G. Gilman, Complexity and diversity of mammalian adenylyl cyclases. *Annu. Rev. Pharmacol. Toxicol.* **36**, 461–480 (1996).
14. W. J. Tang, A. G. Gilman, Type-specific regulation of adenylyl cyclase by G protein beta gamma subunits. *Science* **254**, 1500–1503 (1991).
15. R. Turecek *et al.*, Auxiliary GABAB receptor subunits uncouple G protein $\beta\gamma$ subunits from effector channels to induce desensitization. *Neuron* **82**, 1032–1044 (2014).
16. B. D. Young, J. Sha, A. A. Vashisht, J. A. Wohlschlegel, Human multisubunit E3 ubiquitin ligase required for heterotrimeric G-protein β-subunit ubiquitination and downstream signaling. *J. Proteome Res.* **20**, 4318–4330 (2021).
17. Y. Bayón *et al.*, KCTD5, a putative substrate adaptor for cullin3 ubiquitin ligases. *FEBS J.* **275**, 3900–3910 (2008).
18. M. Brockmann *et al.*, Genetic wiring maps of single-cell protein states reveal an off-switch for GPCR signalling. *Nature* **546**, 307–311 (2017).
19. J. Schwenk *et al.*, Native GABA(B) receptors are heteromultimers with a family of auxiliary subunits. *Nature* **465**, 231–235 (2010).
20. S. Zheng, N. Abreu, J. Levitz, A. C. Kruse, Structural basis for KCTD-mediated rapid desensitization of $GABA_B$ signalling. *Nature* **567**, 127–131 (2019).
21. H. Zuo *et al.*, Structural basis for auxiliary subunit KCTD16 regulation of the $GABA_B$ receptor. *Proc. Natl. Acad. Sci. U.S.A.* **116**, 8370–8379 (2019).
22. M. K. Lobo, E. J. Nestler, The striatal balancing act in drug addiction: Distinct roles of direct and indirect pathway medium spiny neurons. *Front. Neuroanat.* **5**, 41 (2011).
23. A. M. Graybiel, The basal ganglia. *Curr. Biol.* **10**, R509–R511 (2000).
24. T. Nagai, J. Yoshimoto, T. Kannon, K. Kuroda, K. Kaibuchi, Phosphorylation signals in striatal medium spiny neurons. *Trends Pharmacol. Sci.* **37**, 858–871 (2016).
25. A. G. Nair, O. Gutierrez-Arenas, O. Eriksson, P. Vincent, J. Hellgren Kotaleski, Sensing positive versus negative reward signals through adenylyl cyclase-coupled GPCRs in direct and indirect pathway striatal medium spiny neurons. *J. Neurosci.* **35**, 14017–14030 (2015).
26. O. Gokce *et al.*, Cellular taxonomy of the mouse striatum as revealed by single-cell RNA-seq. *Cell Rep.* **16**, 1126–1137 (2016).
27. B. S. Muntean *et al.*, Interrogating the spatiotemporal landscape of neuromodulatory GPCR signaling by real-time imaging of cAMP in intact neurons and circuits. *Cell Rep.* **22**, 255–268 (2018).
28. N. Zhao, A. S. Zhang, C. Worthen, M. D. Knutson, C. A. Enns, An iron-regulated and glycosylation-dependent proteasomal degradation pathway for the plasma membrane metal transporter ZIP14. *Proc. Natl. Acad. Sci. U.S.A.* **111**, 9175–9180 (2014).
29. Y. Zhang, A. Keramidas, J. W. Lynch, The free zinc concentration in the synaptic cleft of artificial glycinergic synapses rises to at least 1 μM. *Front. Mol. Neurosci.* **9**, 88 (2016).
30. W. Maret, Zinc in cellular regulation: The nature and significance of "zinc signals". *Int. J. Mol. Sci.* **18**, 2285 (2017).
31. X. Gao, R. Sadana, C. W. Dessauer, T. B. Patel, Conditional stimulation of type V and VI adenylyl cyclases by G protein betagamma subunits. *J. Biol. Chem.* **282**, 294–302 (2007).
32. J. A. Pitcher *et al.*, Role of beta gamma subunits of G proteins in targeting the beta-adrenergic receptor kinase to membrane-bound receptors. *Science* **257**, 1264–1267 (1992).
33. N. Giordano *et al.*, Motor learning and metaplasticity in striatal neurons: Relevance for Parkinson's disease. *Brain* **141**, 505–520 (2018).
34. B. S. Muntean *et al.*, Gαo is a major determinant of cAMP signaling in the pathophysiology of movement disorders. *Cell Rep.* **34**, 108718 (2021).
35. S. Correale *et al.*, A biophysical characterization of the folded domains of KCTD12: Insights into interaction with the GABAB2 receptor. *J. Mol. Recognit.* **26**, 488–495 (2013).
36. D. M. Pinkas *et al.*, Structural complexity in the KCTD family of Cullin3-dependent E3 ubiquitin ligases. *Biochem. J.* **474**, 3747–3761 (2017).
37. S. Hojyo *et al.*, The zinc transporter SLC39A14/ZIP14 controls G-protein coupled receptor-mediated signaling required for systemic growth. *PLoS One* **6**, e18059 (2011).
38. C. J. Frederickson, S. W. Suh, D. Silva, C. J. Frederickson, R. B. Thompson, Importance of zinc in the central nervous system: The zinc-containing neuron. *J. Nutr.* **130** (suppl. 5S)1471S–1483S (2000).
39. P. Paoletti, P. Ascher, J. Neyton, High-affinity zinc inhibition of NMDA NR1-NR2A receptors. *J. Neurosci.* **17**, 5711–5725 (1997).
40. G. L. Westbrook, M. L. Mayer, Micromolar concentrations of Zn2+ antagonize NMDA and GABA responses of hippocampal neurons. *Nature* **328**, 640–643 (1987).
41. Q. Jiang *et al.*, Characterization of acid-sensing ion channels in medium spiny neurons of mouse striatum. *Neuroscience* **162**, 55–66 (2009).
42. C. Blomeley, E. Bracci, Substance P depolarizes striatal projection neurons and facilitates their glutamatergic inputs. *J. Physiol.* **586**, 2143–2155 (2008).
43. Z. Yan, D. J. Surmeier, D5 dopamine receptors enhance Zn2+-sensitive GABA(A) currents in striatal cholinergic interneurons through a PKA/PP1 cascade. *Neuron* **19**, 1115–1126 (1997).
44. G. Escames, D. Acuña-Castroviejo, J. León, F. Vives, Melatonin interaction with magnesium and zinc in the response of the striatum to sensorimotor cortical stimulation in the rat. *J. Pineal Res.* **24**, 123–129 (1998).
45. K. W. Roche, R. J. O'Brien, A. L. Mammen, J. Bernhardt, R. L. Huganir, Characterization of multiple phosphorylation sites on the AMPA receptor GluR1 subunit. *Neuron* **16**, 1179–1188 (1996).
46. G. Heuschneider, R. D. Schwartz, cAMP and forskolin decrease gamma-aminobutyric acid-gated chloride flux in rat brain synaptoneurosomes. *Proc. Natl. Acad. Sci. U.S.A.* **86**, 2938–2942 (1989).
47. R. F. Krall, T. Tzounopoulos, E. Aizenman, The function and regulation of zinc in the brain. *Neuroscience* **457**, 235–258 (2021).
48. C. Klein, T. Heyduk, R. K. Sunahara, Zinc inhibition of adenylyl cyclase correlates with conformational changes in the enzyme. *Cell. Signal.* **16**, 1177–1185 (2004).
49. M. Ando, N. Oku, A. Takeda, Zinc-mediated attenuation of hippocampal mossy fiber long-term potentiation induced by forskolin. *Neurochem. Int.* **57**, 608–614 (2010).
50. S. L. Sensi *et al.*, The neurophysiology and pathology of brain zinc. *J. Neurosci.* **31**, 16076–16085 (2011).
51. G. Smaldone *et al.*, The BTB domains of the potassium channel tetramerization domain proteins prevalently assume pentameric states. *FEBS Lett.* **590**, 1663–1671 (2016).
52. A. X. Ji *et al.*, Structural insights into KCTD protein assembly and Cullin3 Recognition. *J. Mol. Biol.* **428**, 92–107 (2016).
53. T. Fritzius *et al.*, KCTD hetero-oligomers confer unique kinetic properties on hippocampal GABAB receptor-induced K+ currents. *J. Neurosci.* **37**, 1162–1175 (2017).
54. N. E. Mencacci *et al.*, A missense mutation in KCTD17 causes autosomal dominant myoclonus-dystonia. *Am. J. Hum. Genet.* **96**, 938–947 (2015).
55. B. Al-Mubarak *et al.*, Whole exome sequencing reveals inherited and de novo variants in autism spectrum disorder: A trio study from Saudi families. *Sci. Rep.* **7**, 5679 (2017).
56. C. Golzio *et al.*, KCTD13 is a major driver of mirrored neuroanatomical phenotypes of the 16p11.2 copy number variant. *Nature* **485**, 363–367 (2012).
57. M. T. Lee *et al.*, Genome-wide association study of bipolar I disorder in the Han Chinese population. *Mol. Psychiatry* **16**, 548–556 (2011).
58. K. A. Metz *et al.*, KCTD7 deficiency defines a distinct neurodegenerative disorder with a conserved autophagy-lysosome defect. *Ann. Neurol.* **84**, 766–780 (2018).
59. E. A. Faqeih *et al.*, Phenotypic characterization of KCTD3-related developmental epileptic encephalopathy. *Clin. Genet.* **93**, 1081–1086 (2018).
60. M. Boada *et al.*, Alzheimer's Disease Neuroimaging Initiative, ATP5H/KCTD2 locus is associated with Alzheimer's disease risk. *Mol. Psychiatry* **19**, 682–687 (2014).
61. K. Tuschl *et al.*, Mutations in SLC39A14 disrupt manganese homeostasis and cause childhood-onset parkinsonism-dystonia. *Nat. Commun.* **7**, 11601 (2016).
62. Y. Z. Chen *et al.*, Autosomal dominant familial dyskinesia and facial myokymia: Single exome sequencing identifies a mutation in adenylyl cyclase 5. *Arch. Neurol.* **69**, 630–635 (2012).
63. T. Fuchs *et al.*, Mutations in GNAL cause primary torsion dystonia. *Nat. Genet.* **45**, 88–92 (2013).
64. H. Saitsu *et al.*, Phenotypic spectrum of GNAO1 variants: Epileptic encephalopathy to involuntary movements with severe developmental delay. *Eur. J. Hum. Genet.* **24**, 129–134 (2016).
65. D. Wang *et al.*, Genetic modeling of GNAO1 disorder delineates mechanisms of Gαo dysfunction. *Hum. Mol. Genet.* ddab235 (2021). 10.1093/hmg/ddab235.
66. S. Steinrücke *et al.*, Novel GNB1 missense mutation in a patient with generalized dystonia, hypotonia, and intellectual disability. *Neurol. Genet.* **2**, e106 (2016).
67. K. Lohmann *et al.*, Novel GNB1 mutations disrupt assembly and function of G protein heterotrimers and cause global developmental delay in humans. *Hum. Mol. Genet.* **26**, 1078–1086 (2017).
68. C. P. Diggle *et al.*, Biallelic mutations in PDE10A lead to loss of striatal PDE10A and a hyperkinetic movement disorder with onset in infancy. *Am. J. Hum. Genet.* **98**, 735–743 (2016).